

Nano-Magnetic Hydrotalcite Synthesized by Double In-situ Hydrothermal Method with Enhanced Electromagnetic Characteristics

Li Honglin^{1,2,*}, Ammar Bin Yousaf³, Akif Zeb⁴, Peter Kasak³, Syed Javaid Zaidi³, Li Ying¹, Luo Weiqing¹, Liu Shuaishuai¹, Han Tianli¹, Li Mingling^{1,2}

¹ College of Chemistry and Material Engineering, Chao Hu University, Hefei 238000, China

² Institute of Novel Functional Materials and Fine Chemicals, Chao Hu University, Hefei 238000, China

³ Center for Advanced Materials, Qatar University, Doha 2713, Qatar

⁴ Institute of Environmental Sciences and Engineering (IESE), School of Civil and Environmental Engineering (SCEE), National University of Sciences and Technology (NUST), Sector H-12, Islamabad, Pakistan

*E-mail: lhlin777@163.com

Received: 11 August 2017 / Accepted: 17 September 2017 / Published: 28 December 2017

A series of nano-magnetic hydrotalcite with different content of CoFe₂O₄ is prepared by homogeneous double in-situ hydrothermal method using self-synthesised CoFe₂O₄, Cobalt nitrate hexahydrate (Co(NO₃)₂·6H₂O), magnesium nitrate hexahydrate (Mg(NO₃)₂·6H₂O), nitrate aluminum nonahydrate (Al(NO₃)₃·9H₂O), and sodium hydroxide (NaOH) as starting materials. The crystal structure, morphology, magnetic and thermal stability of the samples were characterized in detail by X-ray diffraction (XRD), scanning electron microscope (SEM), vibrating sample magnetometer (VSM) and thermal gravimetric differential thermal analyzer (TG-DTA) techniques. XRD patterns showed that a small amount of CoFe₂O₄ did not affect the crystallization properties of hydrotalcite, and magnetic hydrotalcite has typical characteristic peak containing both hydrotalcite and CoFe₂O₄. SEM images indicated the magnetic hydrotalcite samples were lamellar with magnetic matrix of CoFe₂O₄ adsorbed on the surface of LDHs layer. The results of VSM displayed that the magnetic hydrotalcite was ferromagnetic, and sample saturation magnetization of three samples increased with the increasing CoFe₂O₄ content with the values of 1.35, 2.7 and 5.9 eum/g. TG-DTA results indicated the thermal decomposition characteristics of magnetic hydrotalcite is similar to the characteristics of pure hydrotalcite thermal decomposition and the addition of magnetic matrix improved the thermal decomposition temperature of the hydrotalcite.

Keywords: hydrothermal; double in-situ; Magnetic; hydrotalcite; structure; properties

1. INTRODUCTION

The combination of magnetic hydrotalcite and magnetic separation is much advantageous for the separation of nanocatalyst and overcomes the problem of recovery of nanocatalyst. The synthesis techniques of magnetic hydrotalcite have become one of the hottest research topics, recently. At present, the synthesis of magnetic hydrotalcite is mostly carried out by chemical coprecipitation and hydrothermal method. Celso, et al. [1] prepared the magnetic nano-MgAlHydrotalcite containing Fe_3O_4 magnetic matrix by chemical coprecipitation method, and studied its adsorption capacity for anions in water. Gabriela, et al. [2] prepared a series of magnetic hydrotalcite as drug-carriers under low supersaturation conditions. Eugenio, et al [3] synthesized NiAl and FeAlHydrotalcite by Coprecipitation method, and studied their intrinsic magnetic properties. Zhang Haiyong, et al. [4] demonstrated that the addition of magnetic matrix did not change the layered structure of hydrotalcite. They synthesised Fe_3O_4 containing Nano-mg-Al Hydrotalcite magnetic matrix with a particle size of 20-50nm by chemical coprecipitation method. Their results also showed that the specific saturation magnetization of the sample increased with the increase of the content of the magnetic matrix. Zhao and Sun Dezhi, et al. [5-6] synthesised a series of magnetic microhydrotalcite-like phosphate adsorbent by chemical coprecipitation method, and studied its adsorption ability for phosphate-containing wastewater. Zhao Wei, et [7], in a similar study, prepared a series of magnetic hydrotalcite-like compounds by chemical coprecipitation. They studied the effects of the composition of magnetic hydrotalcite, molar ratio, pH value and adsorbent dosage on the adsorption properties of phosphate-containing wastewater. Wang, et al. [8-9] synthesised magnetic cobalt aluminum hydrotalcite and Fe_3O_4 matrix by hydrothermal method. Their study showed that the magnetic substrate was successfully incorporated inside hydrotalcite matrix. The magnetic hydrotalcite with hexagonal lamellar structure was relatively uniform. This study showed that the addition of magnetic substrates inhibited the growth rate of hydrotalcite. Sun Rock, et al. [10] studied the effect of magnetic matrix content and calcination temperature on the magnetic properties and structure of Hydrotalcite prepared by hydrothermal method. Zheng, et al. [11-12] prepared a series of magnetic hydrotalcite by chemical coprecipitation and hydrothermal method. The preparation of hydrotalcite by hydrolysis of urea can overcome the colloidal deposition caused by the local concentration of temporary precipitation agent during homogenous coprecipitation method. They found out that this reaction process is easy to control and hence high product crystallinity is achieved [13]. At present the reports on the preparation of magnetic hydrotalcite by homogeneous coprecipitation method are rare. Cheshei, et [14] prepared MFe_2O_4 magnetic nucleus by coprecipitation method for the first time. The magnetic core was mixed with the corresponding salt solution, then the urea-hydrotalcite was gradually grown around the magnetic nucleus, and the homogeneous large-diameter carbonate-type Hydrotalcite containing magnetic cores were obtained.

In the above studies, the synthesis of magnetic matrix and then in-situ synthesis of magnetic hydrotalcite has been analysed. These processes are relatively more complex. In contrast, we have used one step synthesis method in our present study. Magnesium nitrate ($\text{Mg}(\text{NO}_3)_2 \cdot 6\text{H}_2\text{O}$), cobalt nitrate hexahydrate ($\text{Co}(\text{NO}_3)_2 \cdot 6\text{H}_2\text{O}$), ferric nitrate ($\text{Fe}(\text{NO}_3)_3 \cdot 9\text{H}_2\text{O}$), aluminum nitrate ($\text{Al}(\text{NO}_3)_3 \cdot 9\text{H}_2\text{O}$) and sodium hydroxide (NaOH) are used as the main raw materials for double in-situ hydrothermal

synthesis with different content of CoFe_2O_4 to prepare a series of magnetic hydrotalcite ($\text{MgAl-LDHs-CoFe}_2\text{O}_4$). The effect of CoFe_2O_4 content on the properties of magnetic Hydrotalcite are hereby studied. We have found out that, in comparison with the existing methods, our process is simpler and easy to control.

2. EXPERIMENTS

2.1. Materials and Methods

Pure Magnesium nitrate hexahydrate ($\text{Mg}(\text{NO}_3)_2 \cdot 6\text{H}_2\text{O}$), cobalt nitrate hexahydrate ($\text{Co}(\text{NO}_3)_2 \cdot 6\text{H}_2\text{O}$), ferric nitrate ($\text{Fe}(\text{NO}_3)_3 \cdot 9\text{H}_2\text{O}$), aluminum nitrate ($\text{Al}(\text{NO}_3)_3 \cdot 9\text{H}_2\text{O}$), and sodium hydroxide (NaOH) were bought from Nanjing Oriental Chemical Co., Ltd.. Distilled water was prepared in the laboratory on a double distillation system. These chemicals were used as such without any further processing. Glass apparatus were purchased from Tianjin days Glass Instrument co., Ltd, DHG-9053 oven from Wujiang Yun Tatsu Oven Equipment Co., Ltd. Purchase and 50ml teflon autoclave was provided by Anhui Power Machinery Technology Co., Ltd.

2.2. Sample Preparation

The preparation methods of magnetic hydrotalcite ($\text{MgAl-LDHs-CoFe}_2\text{O}_4$) are as follows:

(1) A certain amount of $\text{Co}(\text{NO}_3)_2 \cdot 6\text{H}_2\text{O}$ and $\text{Fe}(\text{NO}_3)_3 \cdot 9\text{H}_2\text{O}$ was added in water (Molar ratio = 1:2) and called solution A. A certain amount of NaOH was added in the water in another beaker (Solution B). Both solutions (A and B) were slowly mixed together (NO_3^- and NaOH molar ratio was 1:2) and heated at 70°C under magnetic stirring for 2 hours. This sample is noted as Sample C. (2) A certain amount of $\text{Mg}(\text{NO}_3)_2 \cdot 6\text{H}_2\text{O}$ and $\text{Al}(\text{NO}_3)_3 \cdot 9\text{H}_2\text{O}$ was added to water (solution D) with a molar ratio of 2:1. A certain amount of solution B was mixed dropwise with solution D while keeping NO_3^- and NaOH molar ratio as 1:2. This solution was heated at 70°C under magnetic stirring for 2 hours and the acquired sample was named as sample E. (3) Sample C and Sample E were added into a teflon autoclave and placed in the oven at 160°C for 10h in oven. The sample was cooled, washed with water and magnetically separated to obtain $\text{MgAl-LDHs-CoFe}_2\text{O}_4$. The molar ratio of Co^{2+} to Mg^{2+} in the solution was 1:70, 1:50 and 1:30 respectively. The samples were noted as sample 1, sample 2 and sample 3. (4) For comparison, a certain amount of sample E was added into teflon autoclave and kept at the same temperature of 160°C in an oven for 10h. The sample was cooled afterwards, washed and dried. MgAl-LDH blank samples were obtained this way. Similarly, a certain amount of precursor C was added into the teflon autoclave and kept at 160°C in oven for 10h, cooled, washed and magnetically separated. The sample was dried and termed as CoFe_2O_4 blank sample.

2.4. Characterization Techniques

Infrared spectroscopic analysis of samples was performed using the Nicolet 5700 Fourier infrared spectrometer (USA-Switzerland Thermo). The sample structure was characterized by the neo-

D Max Japan PC X-ray diffractometer (CuK α =0.15406 nm, 20°/min⁻¹ with a tube current of 40mA tube and voltage of 20kV). The magnetic properties of solid samples were measured via vibrating sample magnetometer (VSM) by the JDAW-2000 type variable temperature vibrating sample magnetometer, (Magnetic torque range 20emu, magnetic field range 2T, magnetic field was set at 10000 Oe with a time constant of 0.1s and demagnetization factor of 0.322). The electromagnetic wave absorption properties (EM) parameters such as, electromagnetic permeability and electromagnetic permittivity were measured by a vector network analyzer (VNA, HP8720ES) in the range of 0–18 GHz. For measurements, the samples were pressed in paraffin homogeneously into toroidal shape with a sample-to-paraffin weight ratio of 1:1, with an inner diameter of ca. 3.0mm, outer diameter of ca. 7.0mm and height of about 3.0 mm. The sample morphology was characterized by JSM 7500F scanning electron microscope (Jeol Japan). The thermal stability analysis of the sample were carried out by the Pyris diamond Tg deta such as, differential scanning calorimetry (DSC) from the temperature of 50-550 °C. Type Thermal weight-difference Thermal Analyzer (American PE company) with a heating rate of 10°/min under the nitrogen atmosphere.

3. RESULTS AND DISCUSSION

3.1 Crystal structure

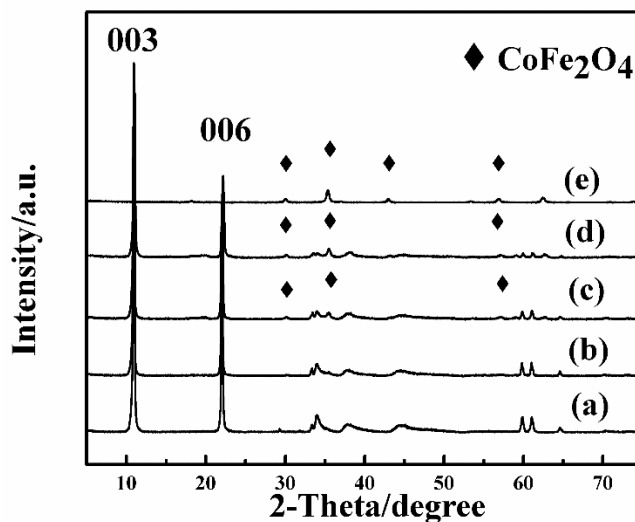


Figure 1. XRD patterns of MgAl-LDH (a), CoFe₂O₄ and Magnetic Hydrotalcite samples with different loadings of CoFe₂O₄ from (b-e).

Figure 1 shows the XRD of CoFe₂O₄, MgAl-LDH and magnetic hydrotalcite samples. It can be seen that the two characteristic peaks of hydrotalcite (11° (003) and 21° (006)) are typical in the samples of magnetic hydrotalcite prepared by double in-situ hydrothermal method. In addition, the XRD pattern shows that the magnetic hydrotalcite samples contains CoFe₂O₄ characteristic peaks. It is also visible from SEM images further, that the magnetic hydrotalcite is still a lamellar structure, and

there is no significant change in the interlayer spacing, proving that the CoFe_2O_4 granule did not enter the MgAl-LDH layer and confirms the results shown in Figure 1.

3.2 Material's Morphology

Figure 2 shows the scanning electron microscope (SEM) images of the blank sample MgAl-LDH and magnetic hydrotalcite (sample 2). From Fig. 2, it can be seen that MgAl-LDH and magnetic hydrotalcite are layered structures. MgAl-LDH surface is smoother as shown in Fig. 2 (A) while magnetic hydrotalcite surface has nanoparticles attached to it (Fig. 2 (B)). The lamellar layer of magnetic hydrotalcite is larger than that of MgAl-LDH sheet. Analysis of magnetic hydrotalcite surface with deposited nanoparticles shows that magnetic matrix with CoFe_2O_4 particles has been successfully prepared.

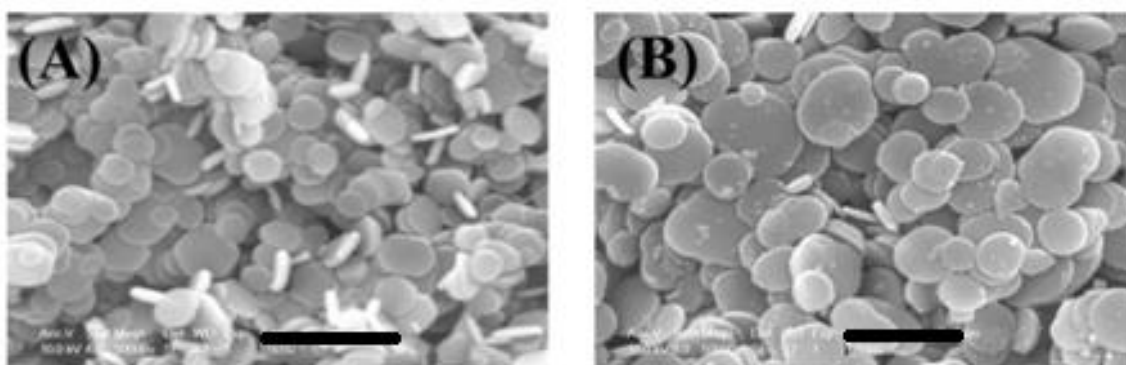


Figure 2. SEM images of MgAl-LDH(A) and Magnetic Hydrotalcite sample 2 (B) with magnification bars of 1 μm .

The size of the magnetic hydrotalcite layer is larger than the MgAl-LDH layer because of the reason that CoFe_2O_4 particles inhibit heterogeneous nucleation and promote the magnetic hydrotalcite grain growth. Figure 3 shows the transmission electron microscope (TEM) images of the magnetic Hydrotalcite (sample 2). It can be seen from Fig. 3, that the magnetic Hydrotalcite sample is of nanometer scale with more than one dimension less than 100 nm.

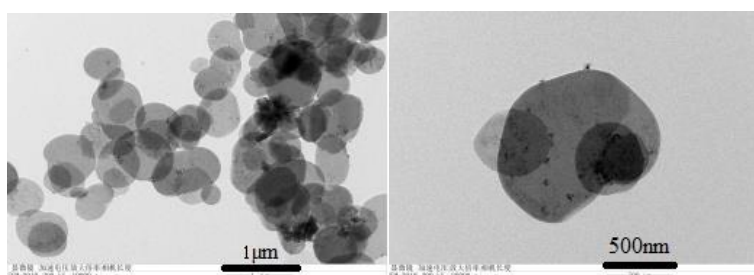


Figure 3. TEM images of Magnetic Hydrotalcite sample 2

3.3 Electromagnetic Characteristics

The electromagnetic behavior of as-developed magnetic materials was tested by magnetic hysteresis loop curves. These magnetization characteristics revealed the potential applications of present materials for electronic recording devices with enhanced performance. In Figure 4, hysteresis loop or electric hysteresis of the magnetic Hydrotalcite sample can be seen. It is found that the samples containing CoFe_2O_4 magnetic hydrotalcite samples prepared by double in-situ hydrothermal method are ferromagnetic.

The y-axis corresponds to the magnetization of samples which measure the extent to which their atomic dipoles aligned with one another by applying electromagnetic field. Whereas, the x-axis corresponds with strength of electromagnetic field and the area between these two axis inside the loop represents the electric hysteresis loose. It is shown from the results that, after removing the external magnetic field the as-developed material retain their magnetization behavior. [15] It is clearly shown that electric hysteresis loose for sample 1 & 2 are lower than that of sample 3, giving a message of superior electromagnetic characteristics of sample 3 than those of other two samples. Furthermore, the specific saturation magnetization of the sample is increased with the increasing content of CoFe_2O_4 with the values of 1.35eum/g, 2.7eum/gand 5.9 eum/g for the sample 1, the sample 2 and the sample 3, respectively.

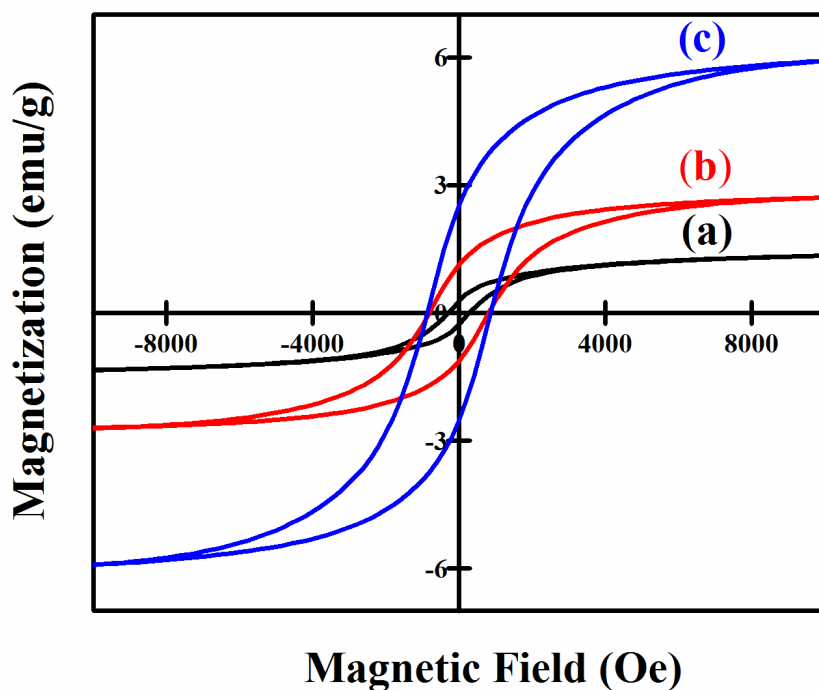


Figure 4. Magnetic Hysteresis loops of Magnetic Hydrotalcite samples such as, (a) sample 1. (b) sample 2 & (c) sample 3.

As it is claimed in morphology and crystal structure discussions that, by adding CoFe_2O_4 in combination with MgAl-LDH in magnetic hydrotalcite, particle size gradually increased. Due to the promotion of magnetic hydrotalcite grain growth the specific saturation magnetization values also

increased. [16] In addition, the effect of double in-situ hydrothermal treatment also affects the improvement in magnetic properties in a way that, by increasing or higher temperatures the rearrangements of cations distribution happen such as, the exchange of Co^{2+} and Fe^{3+} ions from tetrahedral and octahedral sites. [17] Moreover, the ultrafine particles with their large surface to volume ratios in double in-situ hydrothermal treatment may promote the improved electromagnetic behavior of as-developed magnetic hydrotalcite. [18] The obtained magnetic and electromagnetic characteristic improvements in present set of samples are in good agreement with already documented literatures of Fe_2O_4 , Co and CoFe_2O_4 based magnetic materials. [19-23]

Furthermore, the electromagnetic behavior of as-developed magnetic materials was tested by complex magnetic permeability and permittivity for all samples shown in Figure 5. The imaginary parts of the permittivity (Figure 5A) of sample 3 are higher than that of other two samples. In start, after the decrease with increasing frequency, the imaginary part oscillates as a function of the frequency, this trend shown same for all the samples until a longer period. Same as the imaginary part of the permeability, this spectrum fluctuation show the magnetic behavior of the material matrix. The magnetic behavior in the real part follows the same trends for each sample. The linear increase permittivity in imaginary part is observed in sample 3. The real part (u') of magnetic permeability (Figure 5B) increases with increasing frequency upto 3 GHz and reduces to a modest value slightly and then increases again. The resonant peak has not been observed, all the samples show fluctuations of the imaginary part (u'') in accordance with change in frequency. The fluctuations in permeability values may attribute to the eddy current loss of samples due to varying particles clusters size. [24] In the industrial manufacturing systems, the type of matrix and their fabrication technique needed to be considered for tailoring magnetic properties. The relationship between hysteresis and magnetic permeability properties of matrix are used to modify them via the approximation of stress and cluster distributions.

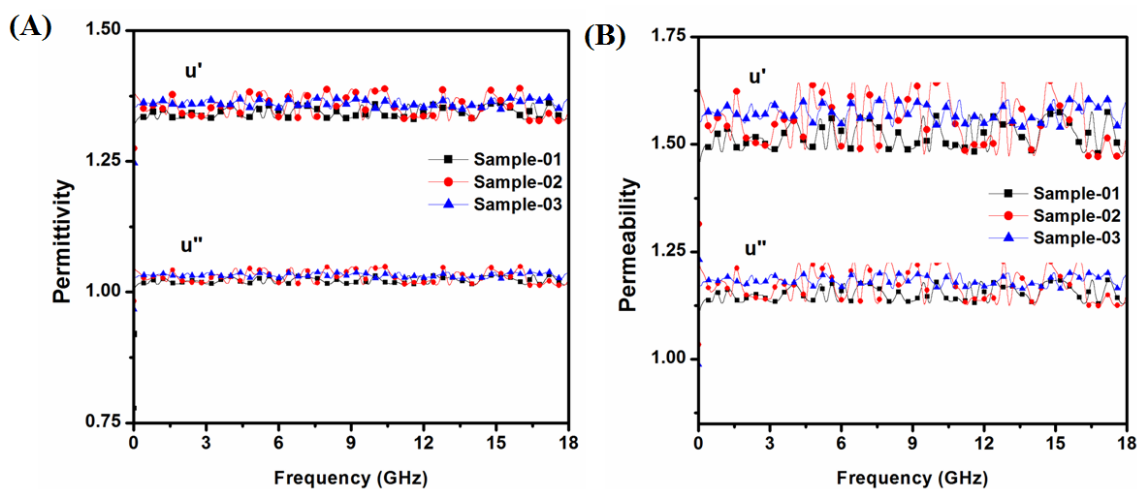


Figure 5. (A) Magnetic permittivity and (B) magnetic permeability spectra for as-prepared samples with their real (u') and imaginary (u'') parts.

3.4 Thermal Stability Analysis

The 3-staged characteristic thermal decomposition of Mg-Al Hydrotalcite and magnetic matrix showed no difference in differential scanning calorimetry (DSC). Fig. 6 shows the thermal weight curve of the magnetic Hydrotalcite sample and the reference sample Hydrotalcite. As evident from Fig. 5, their thermal decomposition process is divided into 3 steps: (1) The loss of weight around 130-160°C corresponds to the removal of small amount of physisorbed water. The weight loss near 210-220 °C corresponds to the removal of the structural carbonate ions and the partial hydroxyl group in the material, and (3) the loss of weight loss within the range of 360-400 °C corresponds to the removal of the hydroxyl groups of the plate material.

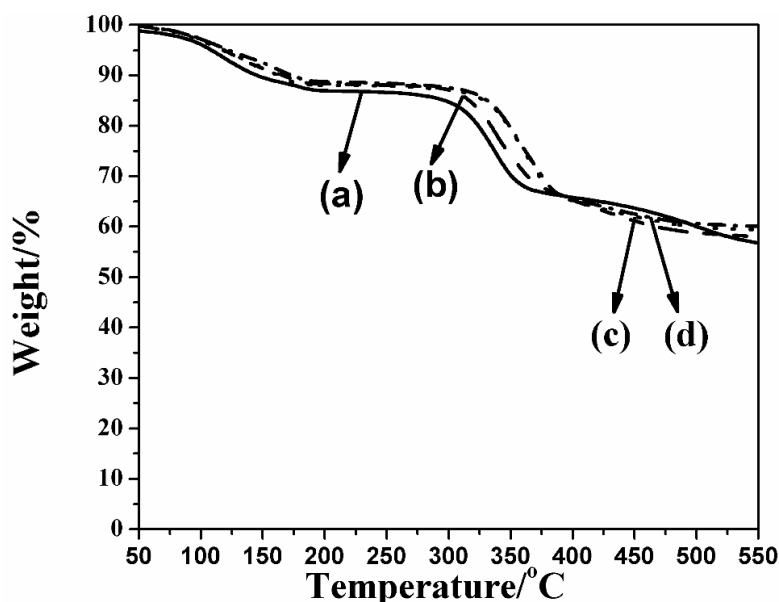


Figure 6. TG Patterns of MgAl-LDH, Sample1, Sample2 and Sample3

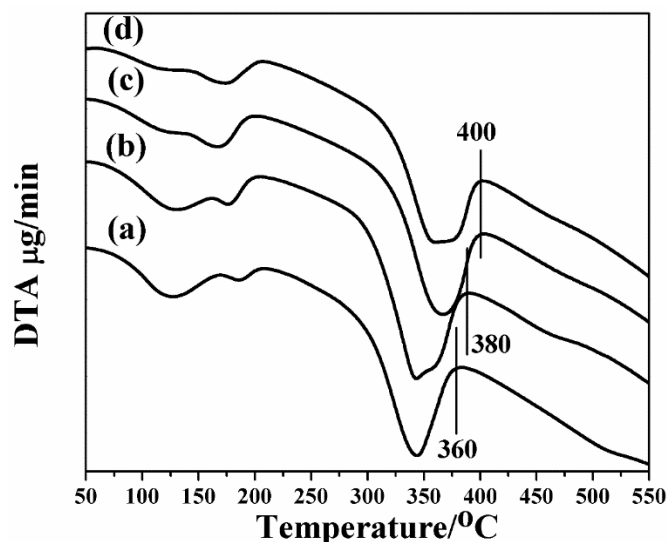


Figure 7. DTA patterns of MgAl-LDH, sample1, sample2 and sample3

It is worth-noting that the removal of hydroxyl group increases with the increase of the content of CoFe_2O_4 magnetic matrix. Henceforth, the thermal decomposition temperature of hydrotalcite can be improved by adding CoFe_2O_4 magnetic matrix. The corresponding DTA curve is shown in Fig. 7.

4. CONCLUSIONS

(1) Magnetic hydrotalcite prepared by double in-situ hydrothermal method is a typical lamellar structure, and the magnetic matrix is uniformly adsorbed on the lamellar surface.

(2) The magnetic hydrotalcite samples prepared by double in-situ hydrothermal method are ferromagnetic, and the saturation magnetization strength increases with the increase of magnetic matrix content.

(3) The thermal decomposition properties of magnetic hydrotalcite samples prepared by double in-situ hydrothermal method are the same as those of pure hydrotalcite samples, while the thermal decomposition temperature of hydrotalcite can be improved by adding magnetic matrix.

ACKNOWLEDGMENT

The author acknowledges the support of outstanding young talent support project for colleges and universities of Anhui province (gxyqZD2016288), Anhui Province University Natural Science Research Project (KJ2015A214) and the national college students innovation training project (201510380002).

References

1. C.M. Celso and C.A.O. Luiz, *Quim Nova*, 31 (2007) 1077-1081.
2. C. Gabriela, C. Horia and L. Nicoleta, *J. Magnetism and Magnetic Materials*, 311 (2007) 26-30.
3. C. Eugenio, G. Jose, M. Carlos, R. Antonio, P. Eli, C. Miguel and B. Ramo, *Inorg. Chem.*, 47 (2008) 9103-9110.
4. H.Y. Zhang, X.Y. Jing, J. Wang, M. Zhang and X. Duan, *Chinese journal of applied chemistry*, 19 (2002) 734-737.
5. B.Q. Zhao, X. Cheng and D. Sun, *Journal of Harbin Institute of Technology*, 12 (2008) 1962-1964.
6. D.Z. Sun, B.Q. Zhao and X.A. Cheng, *J American Chemical Society*, 234 (2007) 74-82.
7. W. Zhao and Y. Chen, *Applied Chemical Industry*, 42 (2013) 450-452.
8. W. Jun, Y. Jia, Z.S. Li, P.P. Yang, X.Y. Jing and M. Zhang, *Nanoscale Research Letters*, 3 (2008) 338-342.
9. J. Wang, J. You, P. Yang, C. Zhong, Z. Li, M. Zhang and X. Jing, *Materials Science-Poland*, 26 (2008) 591-599.
10. W.Y. Sun, C. Zhong, T.F. Liu and Z.S. Li, *Chemical Engineer*, 22 (2009) 7-8.
11. C.H. Zheng, J. Wang and Y.F. Liu, *Chinese Journal of Applied Chemistry*, 24 (2007) 883-886.
12. C.G. Zheng, M. Zhang, J. Wang and X.Y. Jing, *Journal of Harbin Engineering University*, 25 (2004) 803-805.
13. P.P. Yang, M.P. Su and X.W. Yang, *Chinese Journal of inorganic Chemistry*, 19 (2003) 485-490.
14. X. Duan, H. Zhang and K. Zou, *Chinese patent: 200510011996.7*, (2005) 6-24.
15. A. Hunyek, C. Sirisathitkul and P. Jantaratana, *Plastics, Rubber and Composites.*, 42 (2013) 89.
16. K.S. Rao, G. Choudary, K.H. Rao and C. Sujatha, *Procedia Materials Science* 10 (2015) 19-27.

17. R.M. Mohamed, M.M. Rashad, F.A. Haraz and W. Sigmund, *Journal of Magnetism and Magnetic Materials*, 322 (2010) 2058-2064.
18. W.S. Chiu, S. Radiman, R. Abd-Shukor, M.H. Abdullah and P.S. Khiew, *Journal of Alloys and Compounds*, 459 (2008) 291-297.
19. N.M. Deraz and O.H. Abd-Elkader, *Int. J. Electrochem. Sci.*, 10 (2015) 7138-7146.
20. N.M. Deraz and M.M.G. Fouda, *Int. J. Electrochem. Sci.*, 8 (2013) 2682-2690.
21. N. Zhang, Y. Huang, M. Zong, X. Ding, S.P. Li, M.Y. Wang, *Ceramics International*, 42 (2016) 15701–15708.
22. M. Zong, Y. Huang, N. Zhang, *Applied Surface Science*, 345 (2015) 272–278.
23. P. Liu, Y. Huang, X. Zhang, *Materials Letters*, 136 (2014) 298–301.
24. P. C. Fannin, C. N. Marin, I. Malaescu, N. Stefu, P. Vlazan, S. Novaconi, P. Sfirloaga, S. Popescu and C. Couper, *Mater. Des.*, 32 (2011) 1600–1604.

© 2018 The Authors. Published by ESG (www.electrochemsci.org). This article is an open access article distributed under the terms and conditions of the Creative Commons Attribution license (<http://creativecommons.org/licenses/by/4.0/>).